MOLECULAR AND CELLULAR BIOLOGY, Sept. 1993, p. 5549–5559
0270-7306/93/095549-11$02.00/0

Vol. 13, No. 9

Multiple Proteins Interact with the *fushi tarazu* Proximal Enhancer†

WEI HAN, YAN YU, NIHAL ALTAN,‡ AND LESLIE PICK*

Brookdale Center for Molecular Biology, Mt. Sinai School of Medicine, Box 1126, One Gustave L. Levy Place, New York, New York 10029

Received 10 March 1993/Returned for modification 17 May 1993/Accepted 14 June 1993

The expression of the *Drosophila* segmentation gene *fushi tarazu* (*ftz*) is controlled at the level of transcription. The proximal enhancer, located ~3.4 kb upstream of the transcription start site, directs *lacZ* fusion gene expression in a *ftz*-like seven-stripe pattern in transgenic fly embryos. We have taken a biochemical approach to identify DNA-binding proteins that regulate *ftz* gene expression through the proximal enhancer. DNase I footprinting and methylation interference experiments with staged *Drosophila* embryo nuclear extracts identified nine protein binding sites in the proximal enhancer. Ten different sequence-specific DNA-binding complexes that interact with eight of these sites were identified. Some interact with multiple sites, while others bind to single sites in the enhancer. Two of the complexes that interact with multiple sites appear to contain the previously described *ftz* regulators, FTZ-F1 and TTK/FTZ-F2. These in vitro studies allowed us to narrow down the proximal enhancer to a 323-bp DNA fragment that contains all of the protein binding sites. Expression directed by this minimal enhancer element in seven *ftz*-like stripes in transgenic embryos is identical to that directed by the full-length enhancer. Internal deletions of several sites abolish reporter gene expression in vivo. Thus, the *ftz* proximal enhancer, like other cell-type-specific eukaryotic enhancers, interacts with an array of proteins that are expected to mediate the establishment, maintenance, and repression of transcription of the *ftz* gene in seven stripes in the developing embryo.

Extensive genetic and molecular analyses of *Drosophila melanogaster* have identified a large number of genes that establish metameric pattern in the *Drosophila* embryo (1). These genes—maternal coordinate genes, gap genes, pair-rule genes, and segment polarity genes—subdivide the embryo sequentially into increasingly specified regions (17, 18). They are expressed in spatial patterns that correlate with their domains of function during development. The pair-rule genes are the first genes to be expressed in periodically repeated patterns that both preview and determine the repeated metameric patterns of the larval and adult body plans. The pair-rule gene *fushi tarazu* (*ftz*) is expressed in seven stripes that encircle the cellular blastoderm. These stripes are localized to the primordia of the alternating parasegments that are missing in *ftz* mutant embryos (5, 10). Thus, the expression of *ftz*, and other pair-rule genes, in stripes is a prepattern that provides the information for directing the subdivision of the embryo into metameric units. Considerable effort has been directed towards understanding how the striped patterns of pair-rule gene expression are controlled.

Examination of patterns of gene expression in mutant embryos has revealed a molecular hierarchy among the known genes. In general, the expression of genes within each class is dependent upon the wild-type function of genes acting earlier in the hierarchy. The *ftz* expression pattern is altered in embryos carrying mutations in each of the gap genes (5). In addition, genes within a class may regulate each other's expression. The pair-rule genes *runt*, *hairy*, *eve* and *ftz* itself serve to refine and maintain the *ftz* stripes (6, 14, 16). However, with the exception of *ftz* itself (discussed below), it is not known whether any of these genes act directly to regulate *ftz* transcription.

An alternative and complementary approach to analyze regulatory networks during development is to identify proteins present in the early embryo that interact with defined *cis*-regulatory regions. This type of biochemical approach has led to the identification of FTZ-F1 and FTZ-F2/TTK, two previously unknown factors that regulate *ftz* expression via the zebra element (4, 11, 39). In addition, this approach has been used to identify factors regulating *engrailed*, *even-skipped*, and *Antennapedia* gene expression in the developing embryo (2, 29, 31, 35).

The *ftz* gene has been shown to contain three *cis*-acting regulatory elements: the zebra element, the neurogenic element, and the upstream element (Fig. 1) (15). The zebra element directs the expression of a reporter gene, *Escherichia coli lacZ*, in stripes that are restricted to the mesodermal primordia of developing transgenic embryos. The upstream element directs *lacZ* fusion gene expression in stripes via a heterologous promoter. These seven stripes encircle the entire circumference of the embryo at the blastoderm stage, as do endogenous *ftz* stripes (14). The upstream element contains two independent enhancers: the distal enhancer directs expression of seven mesodermally restricted stripes, and the proximal enhancer directs expression in stripes that span both ectodermal and mesodermal primordia (30). Thus, of the three elements involved in stripe formation, the spatial pattern of expression directed by the proximal enhancer most closely resembles that of the endogenous *ftz* gene, which is expressed in stripes at equivalent levels in the ectodermal and mesodermal primordia. The upstream element enhancers direct expression only in stripes; no effect of these elements on *ftz* expression in the nervous system has been observed (14, 30).

Striped expression directed by each of the enhancers is dependent upon the presence of wild-type *ftz* product in the

* Corresponding author.
† Publication 131 of the Brookdale Center for Molecular Biology.
‡ Present address: The Rockefeller University, New York, NY 10021.

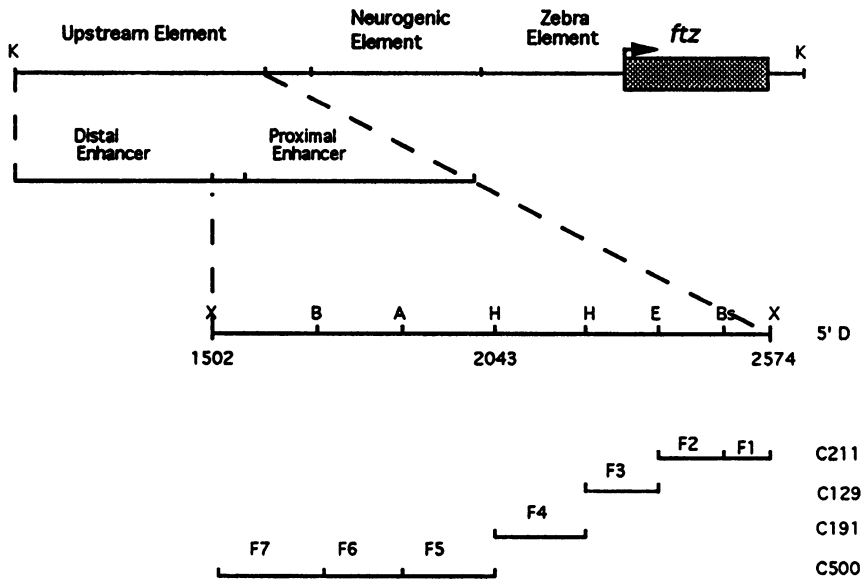

FIG. 1. *ftz* proximal enhancer fragment preparation. The ~6-kb 5'-flanking sequence of the *ftz* gene containing the three previously identified *cis*-acting regulatory elements is shown at the top (14). The zebra element directs *lacZ* fusion gene expression in seven stripes primarily in the mesoderm, the neurogenic element is required for gene expression in neural precursor cells, and the upstream element contains two germ layer-specific stripe enhancers (30) (see Introduction). The distal and proximal enhancers derive from the upstream element. The ~1-kb proximal enhancer *Xba*I fragment (positions 1502 to 2574) is in plasmid DNA construct 5'D (30). The subclones from 5'D are indicated to the right of their respective fragments. Seven fragments, F1 to F7, are indicated. K, *Kpn*I; X, *Xba*I; B, *Bgl*II; A, *Ava*II; H, *Hin*cII; E, *Eco*RV; Bs, *Bst*EII.

embryo, suggesting that they mediate *ftz* autoregulation (14, 30, 34). The differential utilization of the enhancers in the ectodermal and mesodermal primordia led us to propose a minimal model that each of the enhancers requires at least one other factor, in addition to *ftz*, to define its domain of action (30). However, it is more likely that *ftz*—like other transcription factors—acts in a complex involving several proteins. In addition to this well-defined role in autoregulation, the enhancers appear to play a role in stripe establishment (see Discussion).

We have taken a biochemical approach to identify the transcription factors that interact with the *ftz* proximal enhancer to mediate stripe establishment and maintenance. The first step in this analysis is presented here. DNase I protection, methylation interference, and gel retardation assays revealed 9 clustered protein binding sites in the proximal enhancer that interact with 10 different protein complexes present in staged embryonic nuclear extracts. Two of the complexes appear to contain the previously identified proteins, FTZ-F1 and TTK/FTZ-F2, that interact with the zebra element. A 323-bp minimal fragment that contains all of the binding sites directs *lacZ* fusion gene expression in a pattern indistinguishable from that of the intact proximal enhancer.

MATERIALS AND METHODS

***ftz* proximal enhancer fragment preparation.** The seven proximal enhancer fragments shown in Fig. 1 were generated as follows: an *Xba*I fragment (positions 1502 to 2574 of the *ftz* upstream element) (11, 14) in the plasmid XL-7 (29a) was released, gel purified, and cut with *Hin*cII at positions 2043 and 2238, generating three fragments. Fragment 191 (*Hin*cII fragment) was inserted into the *Eco*RV site of the Bluescript KS+ vector, generating subclone C191 (positions 2043 to 2238). Fragment 300 (*Hin*cII-*Xba*I fragment) and 500 (*Xba*I-*Hin*cII fragment) were subcloned into the *Eco*RV and *Xba*I sites of the same vector, giving subclones C300 (positions 2238 to 2574) and C500 (positions 1502 to 2043). C300 was cut with *Eco*RV (position 2363) and *Xba*I; the *Xba*I site of the subclone was filled in with the large fragment of DNA polymerase I, and the two blunt ends were ligated, generating subclone C129 (positions 2238 to 2363). The released *Eco*RV-*Xba*I fragment from C300 was gel purified and ligated to the *Eco*RV-*Xba*I site of a Bluescript KS+ vector, generating subclone C211 (2364 to 2574). F1 and F2 were released from C211 by digestion with *Xba*I and *Eco*RV, respectively, and with *Bst*EII (position 2491). F3 was released from C129 by digestion with *Xba*I and *Hin*dIII. F4 was released from C191 by digestion with *Eco*RV and *Hin*dIII. Fragment 500 was released from C500 by digestion with *Hin*dIII and *Xba*I. The gel-purified fragment was digested with *Bgl*II (position 1718) and *Ava*II (position 1863), generating F5 (*Ava*II-*Xba*I fragment), F6 (*Bgl*II-*Ava*II fragment), and F7 (*Hin*dIII-*Bgl*II fragment). All the *Hin*dIII sites used here are in the polylinker site of the vector. All of the fragments contain at least one 5'-protruding end. All procedures were carried out by standard techniques (22).

Preparation of *Drosophila* embryo nuclear extracts. The procedure used was modified from that of Soeller et al. (35). Embryos (0 to 12 h) were harvested from mass population cages of *D. melanogaster* (Oregon R). The embryos were dechorionated in 3% sodium hypochlorite for 90 s and washed sequentially with 0.7% NaCl–0.04% Triton X-100, 0.7% NaCl, and water. All of the following steps were carried out at 4°C. All solutions used contained the following protease inhibitors: 50 μg of soybean trypsin inhibitor per ml, 1 mM benzamidine, 2 U of aprotinin per ml, 1 μg of antipain per ml, and 1 μg of bacitracin per ml. The embryos were homogenized in homogenization buffer (10 mM *N*-2-

hydroxyethylpiperazine-*N*′-2-ethanesulfonic acid [HEPES; pH 7.5], 25 mM KCl, 0.1 mM spermine, 0.5 mM spermidine-HCl, 1 mM EDTA, 1 M sucrose, 10% glycerol) with ten strokes at 1,000 rpm in a motor-driven Teflon-glass homogenizer. The homogenate was spun at 12,000 rpm for 10 min in a Sorvall SS-34 rotor to remove yolk material. The pellet was resuspended in homogenization buffer and homogenized as before. The homogenate was then layered over a 10-ml cushion containing homogenization buffer-glycerol at a 9:1 ratio. The tubes were spun at 24,000 rpm for 30 min in a Kontron TST28.38 rotor. The nuclear pellet was resuspended in a total volume of 50 ml of lysis buffer (10 mM HEPES [pH 7.5], 0.1 M KCl, 3 mM $MgCl_2$, 0.1 mM EDTA, 10% glycerol), and a 1/10 volume of 4 M ammonium sulfate was added. The tubes were rotated for 30 min and spun at 36,000 rpm for 1 h in a Kontron TFT65.38 rotor. The supernatant was precipitated by addition of 0.3 g of solid ammonium sulfate per ml. After stirring for 15 min, the solution was spun at 36,000 rpm for 25 min in a TFT65.38 rotor. The protein pellets were resuspended in about 50 μl of HEMG (25 mM HEPES [pH 7.5], 0.1 mM EDTA, 12 mM $MgCl_2$, 10% glycerol, 1 mM dithiothreitol) per g of starting material. The protein extract was dialyzed against 2 liters of HEMG plus 40 mM KCl for 2 to 3 h until the conductivity equaled the reading for HEMG plus 0.1 M KCl. To remove precipitated protein, the extract was spun for 30 s in an Eppendorf microcentrifuge. Aliquots were frozen and stored at −80°C.

Gel retardation assay. The procedure was carried out essentially as previously described (7). DNA fragments with 5′-protruding ends were filled in with [α-^{32}P]dATP and the large fragment of DNA polymerase I (Klenow fragment) and purified by using Elutip-d columns (Schleicher & Schuell Co.). Nuclear extract (2 to 6 μg) was incubated with 10 fmol of labeled fragment in a total volume of 25 μl containing 25 mM HEPES (pH 7.6), 0.1 M KCl, 0.5 mM dithiothreitol, 10% glycerol, and 4 to 6 μg of poly(dI-dC) · poly(dI-dC). Samples were kept on ice for 1 h and then electrophoresed at 4°C through 4% native polyacrylamide 0.5× Tris-borate-EDTA (TBE) gels at 12 mA for 1 h with 0.5× TBE as running buffer. Gels were dried after electrophoresis and exposed for autoradiography. For gel retardation with oligonucleotides, nine complementary oligonucleotides were synthesized with the nine fEBC binding site sequences in the center (see boxed regions in Fig. 4) flanked by *Hin*dIII recognition sequences. They were annealed, labeled with [α-^{32}P]dATP as described above, and purified by using Elutip-d columns. The assays were done essentially as described above, except that 2 to 8 μg of random single-stranded oligonucleotide was included in reaction mixtures because of a highly active single-stranded DNA-binding activity present in the nuclear extract that interfered with the assay.

DNase I footprinting assay. The protocol used was modified from that of Ueda et al. (39). Subclones C211, C129, and C191, containing DNA fragments F2, F3 and F4, respectively, were digested with restriction enzymes to generate 5′-protruding ends that were labeled with [α-^{32}P]dATP and the large fragment of DNA polymerase I. The labeled fragments were gel purified. Ten binding reactions were carried out as described above. After the 1-h incubation, 7 μl of 1-U/ml DNase I (Boehringer), 10 μl of 125 mM $MgCl_2$, and 625 mM $CaCl_2$ were added. The digestion on ice proceeded for 1 min and was stopped by the addition of 8 μl of 0.5 M EDTA. The samples were then electrophoresed through native polyacrylamide gels as for the gel retardation assay. After localization of the free probe and protein-probe complexes by autoradiography, the probes were isolated from gel slices by electroelution. The DNA was purified by extraction with an equal volume of phenol-chloroform (1:1), extraction with chloroform, passage over an Elutip-d column, and precipitation with ethanol. Equal amounts of radioactivity from the bound and free DNA probes were separated on 8.3 M urea–8% polyacrylamide gels in 1× TBE with guanine cleavage reactions as markers (23). The gels were exposed for autoradiography after being dried.

Methylation interference assay. The methylation interference assay was done essentially as described by Hendrickson and Schleif (13). The DNA fragments F2, F3, and F4 were end labeled as described above and partially methylated with dimethyl sulfate (24). The methylated fragments were then incubated with nuclear extract under the same conditions described above. After separation of free and bound fragments on native gels, each was electroeluted from a gel slice. The DNA was purified as described above, cleaved at the methylated guanine sites with piperidine treatment (24), and electrophoresed through 8.3 M urea–8% polyacrylamide gels in 1× TBE buffer. The gels were exposed for autoradiography after they were dried.

***ftz*-proximal enhancer-*lacZ* fusion genes.** The fusion gene constructs are shown in Fig. 8. To generate Prox 531, a 531-bp *Xba*I fragment (positions 2043 to 2574 of the upstream element) was excised from Rev 2043 (30) and inserted into the *Xba*I site of the Bluescript KS+ vector. Deletion constructs were created by cleavage with enzymes that remove an internal fragment of the enhancer but do not cleave the vector. After cleavage, overhangs, if present, were filled in with the large fragment of DNA polymerase I and the vector was religated. The 5′ deletion (Prox 406) was created by digesting Prox 531 with *Dra*I and *Xba*I (positions 2043 and 2168). To make the 3′ deletion (Prox 323), Prox 406 was digested with *Bst*EII and *Xba*I (positions 2491 and 2574). To generate internal deletions, the 531-bp proximal enhancer fragment (positions 2043 to 2574) was inserted into the *Xba*I site of pUC19. Deletion endpoints were 2323 and 2491 (*Mlu*I and *Bst*EII), 2366 and 2491 (*Eco*RV and *Bst*EII), and 2309 and 2421 (*Sty*I). All enhancer fragments (see Fig. 8) were subcloned into the *Xba*I site of HZ50PL (14). HZ50PL contains the *E. coli lacZ* gene as a reporter driven by a basal *hsp70* promoter, a *rosy* gene as eye color marker, and P-element borders to allow for integration into the *Drosophila* germ line. *ftz-lacZ* fusion genes were coinjected with the helper plasmid p25.1WC into ry^{506} embryos by standard procedures (33, 36). Following transformation into the germ line of *D. melanogaster*, at least five independent lines were established for each fusion gene. Fusion gene expression in embryos was monitored by immunohistochemical staining of whole-mount embryos by modifications of standard protocols (9a). The anti-β-galactosidase antibody was from Cappell. ABC reagents from Vector Laboratories were used for visualization. Embryos were photographed by using Nomarski optics on a Zeiss Axiophot microscope with TMAX-100 film.

RESULTS

The proximal enhancer contains a cluster of nuclear protein binding sites. Nuclear extracts were prepared from freshly collected 0- to 12-h *Drosophila* embryos by a modification of the method of Soeller et al. (35). Each extract was tested for in vitro transcription activity by using the *ftz* promoter as a template to ensure optimal solubilization and preparation of nuclear factors (data not shown).

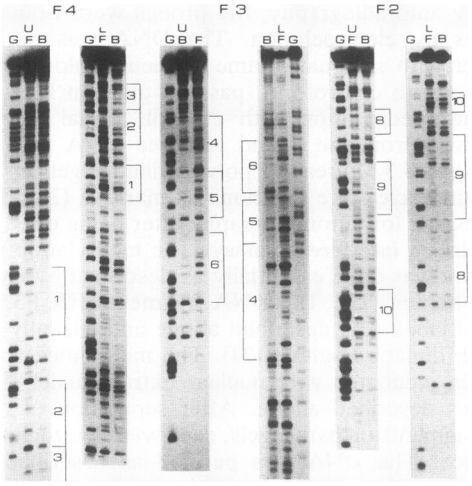

FIG. 2. Nuclear proteins interact with multiple sites in the proximal enhancer. The *ftz* enhancer fragments F2, F3, and F4 were ^{32}P labeled on either the upper (U) or the lower (L) DNA strand and used as probes in DNase I footprint assays (see Materials and Methods). Autoradiographs of 8% sequencing gels are shown for both strands of each probe. The digested fragments from the DNA-protein complexes are shown in lanes B (bound) and the free probes are in lanes F. Lanes G (guanine): sequences of the fragments are from Maxam-Gilbert sequencing reactions. The footprint sites are indicated by numbered bars along both strands.

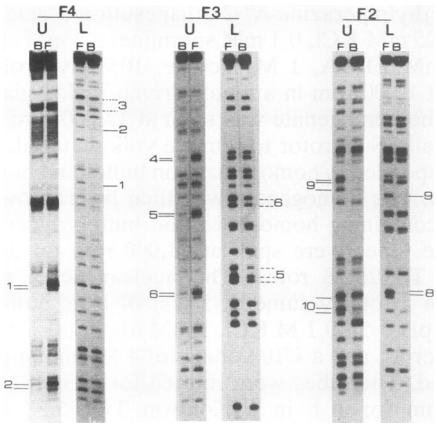

FIG. 3. Methylation interference analysis of the *ftz* proximal enhancer. Autoradiographs of sequencing gels showing chemical cleavage at sites of methylated guanine on both the upper (U) and lower (L) strands of the *ftz* proximal enhancer fragments (F4, F3, and F2) are shown. The digested fragments from the protein-DNA complexes are shown in lanes B (bound), and the free probes are in lanes F. The lines and dotted lines indicate guanine sites which, when methylated, interfered with protein binding (see Materials and Methods). The dotted lines are weak interference sites. The numbers beside the lines indicate the respective footprint sites (Fig. 2) in which the detected guanines are located.

To screen for proteins that interact with the *ftz* enhancer region, the proximal half (~1 kb) of the upstream element (14) was divided into seven regions (~100 to 200 bp each; F1 to F7), as shown schematically in Fig. 1. In gel retardation assays, only fragments F2, F3, and F4 generated specific protein-DNA complexes (one complex per fragment [data not shown]). This localized the specific protein-DNA interactions to the proximal portion (~0.5 kb) of the proximal enhancer between positions 2043 and 2489.

To further characterize binding sites in this region, DNase I footprint analysis was carried out by using the three fragments as probes. As shown in Fig. 2, proteins in the nuclear extract protected three regions on each fragment from DNase I digestion. All footprinted regions were confirmed on both strands (Fig. 2). These footprinted regions are numbered 1 to 6 and 8 to 10, with site 7, a nonfootprinted region (positions 2121 to 2140), serving as a negative control. Most of the protected regions are small (10 to 14 bp), suggestive of an interaction with a single protein. Sites 6 and 8 are slightly larger (25 bp), and one more-extensive region (spanning sites 4 and 5) was detected, suggesting that multiple proteins interact with these sequences.

To identify potential direct protein-DNA contact sites within the footprinted regions, methylation interference analysis was carried out. DNA fragments F2, F3, and F4 were each methylated after end labeling and incubated with nuclear extract. After separation through native gels, the shifted complexes and free probes were excised and subjected to chemical cleavage at guanine sites. Products were separated on denaturing gels, as shown in Fig. 3. Guanine residues whose methylation interfered with binding were identified for each footprinted region; no sites were found outside of the footprinted regions.

A summary of the DNase I protection and methylation interference assays is shown in Fig. 4. A striking feature of the sites is that each contains the sequence AGGA, which is the part of the consensus sequence of TTK/FTZ-F2 binding sites (4). Methylation interference assays indicate that, in all but one case (within site 4), the GG in this consensus is in close contact with a protein. However, two AGGA sites (positions 2363 to 2366 and 2283 to 2286) were not detected by methylation interference. In addition, the methylation interference patterns and DNA sequences lying outside of the AGGA core vary from site to site. A second consensus sequence found among four footprinted regions is CAAGGA, part of the consensus sequence for the protein FTZ-F1, which was shown to interact with the *ftz* zebra element (39). This sequence is present in sites 4, 6, 8, and 9.

In sum, these experiments identified nine regions clustered within the proximal ~300 bp of the proximal enhancer that interact with proteins present in embryonic nuclear extracts. Although the sites all contain AGGA, the pattern of methylation interference and the diversity of the regions outside of this sequence suggest that different proteins interact with different sites in the enhancer.

Multiple proteins interact with the proximal enhancer. To further characterize the binding activities that interact with the footprinted sites, we carried out gel retardation assays with double-stranded oligonucleotides as probes. Ten oligonucleotides corresponding to each site (Fig. 4) and to one nonfootprinted site, as a control, were synthesized. Binding conditions were varied to determine the optimal conditions for complex formation. These studies revealed the presence of a highly active single-stranded DNA-binding activity in the extract that interacted with every oligonucleotide. This activity was effectively inhibited by the addition of 0.1 μg of any single-stranded oligonucleotide to the reaction mixtures. Protein-DNA complexes were identified for all oligonucleotides tested except for the control site (site 7). In addition, no shifted complex was detectable with oligonucleotide 10 (O10) under any condition tested.

Cross-competition among the oligonucleotides was carried out in the gel retardation assays to determine the specificity

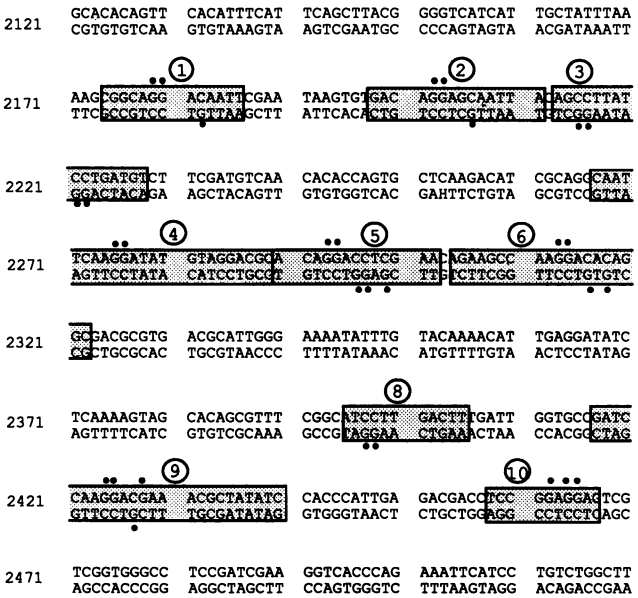

FIG. 4. Summary of nuclear protein binding sites in the *ftz* proximal enhancer. A 400-bp region of the *ftz* proximal enhancer (positions 2121 to 2520) is shown. Nine sites were identified by DNase I footprinting of this region by using 0- to 12-h *Drosophila* embryonic nuclear extract (Fig. 2). The shaded boxes are the footprint sites numbered in circles above them (1 to 6 and 8 to 10). Site 7 (positions 2121 to 2140), a randomly chosen nonfootprinted region used as a negative control, is not indicated. Dots indicate the guanine residues which were detected by methylation interference assays. The exact borders of adjacent footprint sites were assigned on the basis of gel retardation experiments (see below) using different oligonucleotides that overlap with different portions of the footprinted regions (data not shown).

of each DNA-binding activity—*ftz* enhancer binding complex or fEBC (Fig. 5). As shown in Fig. 5A, the two shifted complexes generated with O2 were specific to O2 (lane 1); a 50-fold molar excess of unlabeled O1, O3, O4, O6, O8, O9, or O10 failed to inhibit the binding, while the complexes were abolished in the presence of the same amount of unlabeled O2. Similarly, fEBC3 (Fig. 5B) was specifically inhibited by O3 only. The situation for fEBC4 to 7 (Fig. 5C) was somewhat more complex because of the complexity of the binding pattern itself. Complexes fEBC4 and -7 were completely abolished only by excess O4; however, the other oligonucleotides (except O10) led to somewhat reduced binding, suggesting that fEBC4 and -7 protein(s) have lower affinity for these sequences. Formation of complex fEBC5 was inhibited by O4, O9, and more weakly by O6, whereas formation of fEBC6 was inhibited only by O4. Thus, several distinct protein complexes interact with O4, consistent with the large size of its DNase I-protected region.

As shown in Fig. 5D, the three complexes that interact with O6 have distinct competition patterns. Complexes fEBC8 and -9 were resistant to a 50-fold molar excess of O1, O2/3, O5, and O10. The more rapidly migrating complex fEBC10 was efficiently inhibited by all oligonucleotides, although O10 appeared to be the weakest competitor. O4 and O8 competed for fEBC8 and -9 complex formation less efficiently than O6 and O9. Consistent with this observation, the binding and competition patterns with O9 as a labeled probe were identical to those shown for O6 (data not shown). Similar cross-competition patterns for O1, O5, and O8 confirmed the findings shown here. O1 and O5 generated only fEBC10 (see also Fig. 7B, lane 2, and 7A, lane 3), while fEBC8 and -10 were detected with O8 (see Fig. 6B, lane 4).

In sum, gel retardation assays with single oligonucleotides corresponding to sites identified by footprint and methylation interference analysis revealed an array of DNA-binding activities that interact with the proximal enhancer. A summary of the specific protein-DNA complexes identified is shown in Fig. 5E. Some of the complexes interact with unique regions in the enhancer: fEBC1 and -2 with O2, fEBC3 with O3, and fEBC4 to 7 with O4. Others interact with multiple sites: fEBC9 with O6 and O9; fEBC8 with O6, O8, and O9; and fEBC10 with at least five sites (O1, O5, O6, O8, and O9). Although footprint site 10 showed clear footprint and methylation interference patterns, no complex was identified in gel retardation assays with this oligonucleotide. This suggests that proteins interacting with this region bind cooperatively with proteins interacting with other sites in the enhancer. The negative control O7 failed to produce any complexes in the gel retardation assay.

Complexes fEBC8 and -10 contain the *ftz* regulatory proteins FTZ-F1 and TTK/FTZ-F2. Since proteins in fEBC8, -9, and -10 interact with several protein binding sites in the enhancer, consensus sequences could be derived for these complexes. They are AGGA for fEBC10, CAAGGA for fEBC8, and CCAAGGAC for fEBC9 (Fig. 4). These sequences suggested that fEBC10 might contain the DNA-binding protein TTK/FTZ-F2 (4, 12) and that fEBC8 might contain the previously identified *ftz* regulator FTZ-F1 (20, 39).

To test for the presence of FTZ-F1 binding activity in the complexes, we did gel retardation assays with an oligonucleotide containing a known FTZ-F1 binding site 1 (39) as a competitor. As shown in Fig. 6A, an excess of FTZ-F1 binding site 1 (lane 2) efficiently competed for fEBC8 and 9 complex formation with O6. Addition of anti-FTZ-F1 antibody to the reaction mixtures abolished the formation of fEBC8, but fEBC9 was unaffected (Fig. 6B, lanes 2 and 5). Addition of preimmune serum had no effect on complex formation (Fig. 6B, lanes 3 and 6). The same results were obtained by using O9 as a labeled probe (data not shown). Addition of any of the sera to gel retardation reaction mixtures generated a slowly migrating species that was not dependent upon the addition of nuclear extract (Fig. 6B, lanes 7 and 8). These results suggest that although fEBC8 and -9 are formed with similar DNA sequences, they contain distinct proteins and that fEBC8 contains FTZ-F1 (see Fig. 5E and Fig. 10).

Similar experiments were carried out to test for the presence of TTK/FTZ-F2 protein in the complexes. As shown in Fig. 7A, formation of fEBC10 with O5 (lane 3) was completely abolished by the addition of anti-TTK antibodies to the binding reaction mixture (lane 2) but was unaffected by the addition of preimmune serum (lane 1). As shown in Fig. 7B, the mobility of fEBC10 (lane 2) was identical to that generated by incubation of the same oligonucleotide with TTK protein synthesized in *E. coli* (kindly provided by D. Read) (lane 1). The same results were obtained for fEBC10 complex formation with O1, O6, O8, and O9. Furthermore, the addition of anti-TTK antibodies to binding reaction mixtures with O2 and O3, which do not generate fEBC10 (Fig. 5), had no effect on complex formation (data not shown). As shown in Fig. 7C, complexes failed to form with bacterially expressed TTK protein and oligonucleotides containing mutations in the core sites of O6, O5, and O1 (M6, M5, and M1, respectively). Similarly, fEBC10 complex

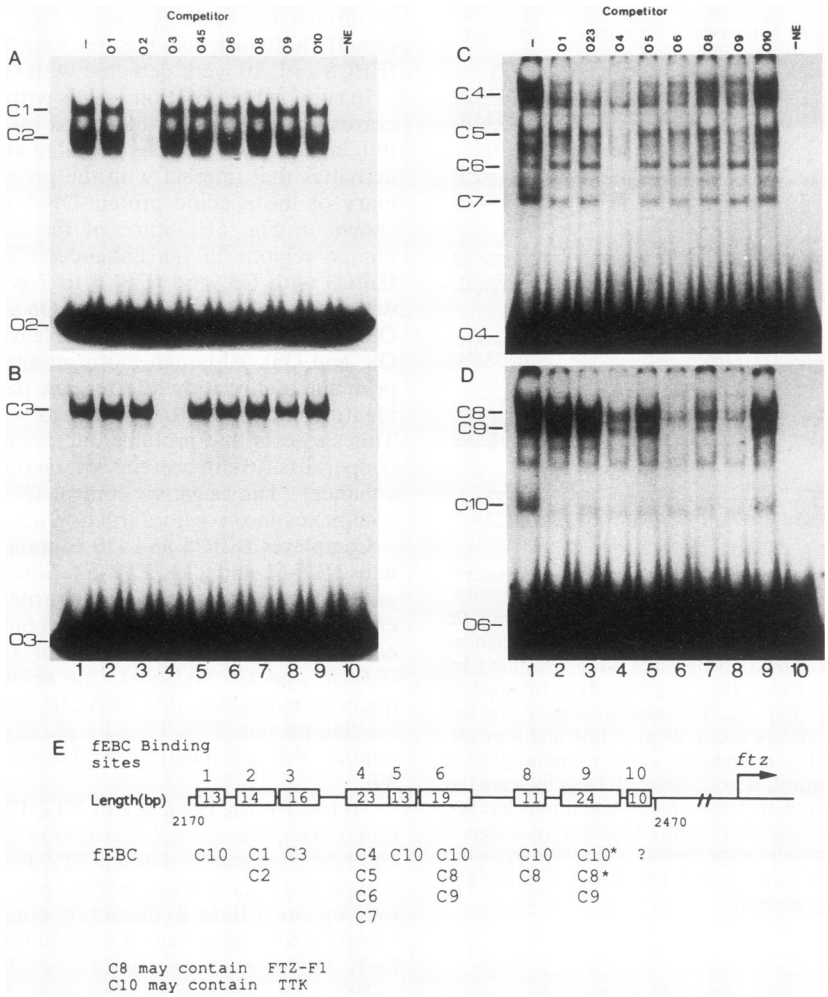

FIG. 5. Specific proteins interact with the *ftz* proximal enhancer. Nine double-stranded oligonucleotides (O1 to O6 and O8 to O10) containing the DNA sequences of the nine footprint sites (boxed in Fig. 4) were synthesized. The names correspond to the numbers of their respective footprint sites (Fig. 4). Four representatives of the nine oligonucleotide gel retardation assays are shown. The same competitors and lane numbers were used for panels A and B and for C and D. Lanes 1, no competitor; lanes 10, no nuclear extract (NE); lanes 2 to 9, a 50-fold molar excess of the indicated unlabeled oligonucleotide was used as competitor. O45 is an oligonucleotide containing the sequences covering footprint sites 4 and 5; O23 covers the footprint sites 2 and 3. O2, O3, O4, and O6 on the left of the panels indicate the free oligonucleotide probes. *ftz* enhancer binding complexes fEBC1 (C1) to fEBC10 (C10) are 10 different slowly migrating protein-oligonucleotide complexes. Two nonspecific complexes were detected when O4 was used as probe (C). Below fEBC4 is a single nonspecific species that is not inhibited by any oligonucleotide, including O4. In addition, a species migrating between fEBC5 and -6 corresponds to residual single-stranded DNA-binding activity, described in the text. Similarly, the complex between fEBC9 and -10 is nonspecific (D). (E) A diagrammatic representation of fEBCs interacting with the *ftz* proximal enhancer. Nine fEBC binding sites are indicated above a 400-bp region of the *ftz* proximal enhancer. All protein binding sites were located in a region of the enhancer between positions 2470 and 2170. C1 to C10 represent 10 fEBC1 to -10 grouped below their respective binding sites. No binding activities were detected at fEBC10 (?) by gel retardation assays. All complexes were stable in up to 0.3 M NaCl in the presence of 4 μg of poly(dI · dC) · poly(dI-dC). The asterisks indicate that C8 may contain FTZ-F1 (20) and that C10 may contain TTK protein (12).

formation with nuclear extract was not detected with the mutated oligonucleotides (shown for O5 only [Fig. 7D]). These results strongly suggest that fEBC10 protein corresponds to *Drosophila* TTK/FTZ-F2 (see Fig. 5E and Fig. 10).

The region containing clustered fEBC binding sites is sufficient to direct *lacZ* fusion gene expression in transgenic flies. The proximal enhancer was previously defined as a 794-bp fragment (positions 1780 to 2574) that directs *lacZ* fusion gene expression in seven *ftz*-like stripes via a heterologous promoter in transgenic embryos (Fig. 8). As shown in Fig. 9A, a smaller fusion gene, Prox 531 (positions 2043 to 2574), was expressed in seven *ftz*-like stripes indistinguishable from the original 794-bp proximal enhancer. Since no binding sites for nuclear proteins were identified in the 5′-most 125 bp of this fragment, that region was deleted from Prox 531. As shown in Fig. 9B, this deletion (Prox 406) caused no change in the striped expression pattern. Similarly, the 83 bp at the 3′ end of Prox 406 which contains no fEBC binding site was deleted (Prox 323). As shown in Fig. 9C, this 83-bp region was also dispensable for striped expression. Thus, the 323-bp region defines a minimal proximal enhancer fragment that contains all identified fEBC binding sites and is sufficient to direct *ftz*-like striped expression in the developing embryo.

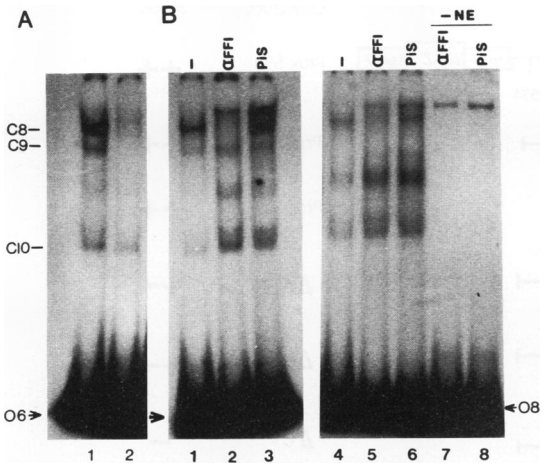

FIG. 6. fEBC8 may contain FTZ-F1. (A) Probe O6 was ^{32}P labeled and incubated with 0- to 12-h *Drosophila* nuclear extract (NE). A 50-fold molar excess of an oligonucleotide containing FTZ-F1 binding site I (5′-GTCGACGCAGCACCGTCTCAAGGTC GCCGAGTAGGAGAA-3′) (39) specifically inhibits fEBC8 (C8) and fEBC9 (C9) binding to O6 (lane 2) in gel retardation assays. (B) Gel retardation assays were carried out with oligonucleotides O6 and O8 (lanes 1 and 4) in the presence of 2 μl of anti-FTZ-F1 antibody (αFF1 [lanes 2, 5, and 7]) or 2 μl of preimmune serum (PiS [lanes 3, 6, and 8]). Anti-FTZ-F1 antibody, but not preimmune serum, specifically abolished fEBC8 binding to O6 and O8. fEBC9 complex formation with O6 was not affected by addition of antibodies. −NE, no nuclear extract added. fEBC8 (C8), fEBC9 (C9), and fEBC10 (C10) refer to both panels.

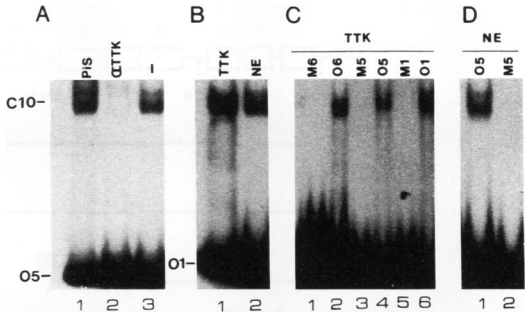

FIG. 7. fEBC 10 may correspond to TTK/FTZ-F2. (A) Autoradiograph showing a gel retardation assay with ^{32}P-labeled O5 (lane 3), with 2 μl of anti-TTK/FTZ-F2 antibody (αTTK [lane 2]), or with 2 μl of preimmune serum (PiS [lane 1]). Anti-TTK/FTZ-F2 antibody abolished fEBC10 (C10) binding to O5. (B) Gel retardation assay with O1 and different protein sources. Lane 1, 0.2 μg of bacterially expressed TTK/FTZ-F2; lane 2, 4 μg of 0- to 12-h *Drosophila* nuclear extract (NE). (C) Bacterially expressed TTK/FTZ-F2 (0.2 μg) was incubated with ^{32}P-labeled wild-type O6, O5, and O1 or corresponding mutant oligonucleotides M6, M5, and M1 in gel retardation assays. TTK/FTZ-F2 did not bind to the mutant oligonucleotides. The sequences of the mutant oligonucleotides were as follows: M1, CGGCGATAGTTCTCG; M5, ACAT CAGATAGAA; and M6, AGAAGCCAGATATGAAGGC. (D) Nuclear extract (NE; 4 μg) was incubated with probe O5 (lane 1) or M5 (lane 2) and analyzed by gel retardation.

Internal deletions of the minimal proximal enhancer had strong effects on expression. Fusion gene ΔA, which removes 125 bp, and fusion gene ΔB, which removes 168 bp, are each expressed extremely weakly (Fig. 9D and E), although the two are expressed at roughly equivalent levels. Each of these deletions removes the enhancer binding sites O8, O9, and O10, suggesting that some or all of these sites are involved in directing gene expression in vivo. A third internal deletion (ΔC) of 112 bp removes binding sites O6, O8, and O9. No expression of this fusion gene (Fig. 9F) was detected in transformant embryos, suggesting that these sites, each of which interacts with proteins in complexes fEBC8, -9, and -10, are essential for gene expression in the embryo.

DISCUSSION

We have taken a biochemical approach to identify transcription factors that regulate *ftz* transcription during *Drosophila* embryogenesis. Nuclear extracts were prepared from 0- to 12-h embryos and used for DNase I footprinting, methylation interference, and gel retardation assays to identify proteins that interact with the *ftz* proximal enhancer. This analysis localized nine protein binding sites within ~300 bp of the enhancer, as summarized in Fig. 4, 5E, and 10. This fragment, but not internal deletions thereof, directed *ftz-lacZ* fusion gene expression in a *ftz*-like seven-stripe pattern in transgenic embryos. Cross-competition among oligonucleotides corresponding to each binding site in the enhancer indicated that 10 distinct protein complexes interact with the nine sites. Some of these complexes were unique to a single DNA region; others were formed repeatedly with several oligonucleotides. Of the complexes identified, one (fEBC8) appears to contain the previously identified *ftz* regulator, FTZ-F1, which binds to three sites in the enhancer. Another complex (fEBC10) appears to correspond to TTK/FTZ-F2, which binds to at least five regions in the enhancer.

Complicated organization of the *ftz* proximal enhancer. Although the large number of binding sites and protein-DNA complexes identified is surprising at first glance, this complexity is actually typical of eukaryotic enhancers examined to date. For example, the immunoglobulin H intron (37) contains a 700-bp enhancer (ENH_{IH}) that functions as a potent B-cell-specific enhancer. It contains 16 protein binding sites; 15 DNA-binding proteins that interact with 11 of the 16 sites have been identified. Some of the sites were bound by multiple proteins, e.g., the octamer site was bound by three proteins (oct-1, oct-2, and oct-3); some of them interact with only one protein, e.g., the E site was bound by only Ig/EBP-1. Among the proteins characterized, most of them interact with only one site, but NF-μNF interacts repeatedly with four binding sites (P1 to P4). Mutation analysis indicated that the multiple sites are functionally redundant and that they regulate gene expression both positively and negatively.

An enhancer of a developmentally regulated gene such as *ftz* would be expected to be at least as complex as this. Multiple factors are required for the establishment, maintenance, and repression of the seven *ftz* stripes. Two *cis*-regulatory regions that control stripe expression have been identified. The zebra element (+1 to ~−700) directs *lacZ* fusion gene expression in seven mesodermally restricted stripes and contains multiple activator and repressor elements that have been characterized in some detail (8, 9, 38). Further upstream is a region (the upstream element, −3.4 to −6 kb) (14) containing two independent enhancers (30). Both qualitative and quantitative data indicate that the enhancers are required, in conjunction with the zebra element, for stripe establishment. The proximal enhancer is the only regulatory element that directs expression in stripes that

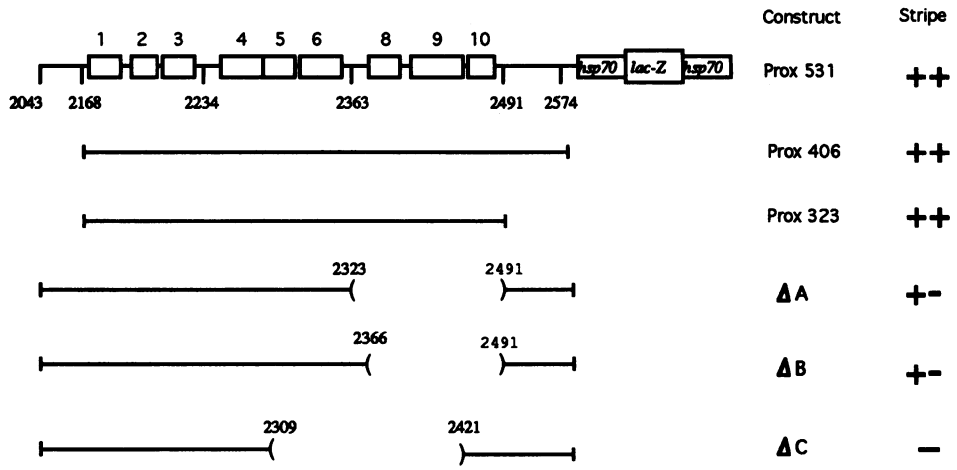

FIG. 8. *ftz* proximal enhancer-*lacZ* fusion genes. The *ftz* proximal enhancer was fused to the reporter gene *lacZ*, which is driven by a basal *Drosophila hsp70* promoter in the P-element transformation vector HZ50PL (14). The numbering system for the *ftz* proximal enhancer is from Harrison and Travers (11). The boxes represent the fEBC binding sites which are numbered above them. DNA constructs Prox 406 and Prox 323 are deletions of Prox 531. ΔA, ΔB, and ΔC are internal deletions of Prox 531 with the deletion positions indicated (see Materials and Methods). The *lacZ* expression of the DNA constructs is summarized at the right: ++, *ftz*-like seven stripes; +−, weak stripes; −, no expression detectable.

surround the entire circumference of the embryo at the blastoderm stage, as does the endogenous *ftz* gene. Stripes directed by either the zebra element or the distal enhancer are expressed primarily on the ventral side of the embryo, in the mesodermal primordia. Thus, the proximal enhancer is necessary for the correct spatial expression of *lacZ* fusion genes. In addition, the level of expression in stripes directed by the zebra plus upstream elements are greater than additive (8, 14), suggesting an interaction between the elements in stripe establishment.

The role of the proximal enhancer in mediating stripe maintenance via autoregulation has been well documented. Expression of enhancer-*lacZ* fusion genes is responsive to *ftz* product in vivo and multiple binding sites for *ftz* protein have been identified in the enhancer (see below). Despite the fact that expression is maintained by a positive autoregulatory feedback loop, stripes decay rapidly in the embryo. Although nothing is known about this process, the rapidness of stripe decay suggests that autoregulation is actively repressed and that sites in the enhancer(s) are required for this repression. It has been proposed that *ttk* product plays a role in this process (12).

The nuclear extracts used here contain factors from all cells in the embryo, both during the phase that *ftz* is transcribed (1 to 6 h) and for several hours thereafter. Thus, it is likely that these extracts contain factors active in establishment, maintenance, and repression of stripes both spatially and temporally. Different factors may interact with the same binding sites in different cells and at different times of development. This array of interactions required to direct *ftz* expression may explain the multiple complexes identified in our studies. In particular, the multiple complexes that interact with single sites (e.g., the complexity of binding to O4) may result from a reutilization of binding sites at different stages of *ftz* stripe development in the embryo. The role that each binding site plays in *ftz* expression in vivo is currently being examined by site-directed mutagenesis. However, since the nuclear extracts are also expected to contain factors that do not regulate *ftz* expression in the embryo, demonstration that any of the identified complexes

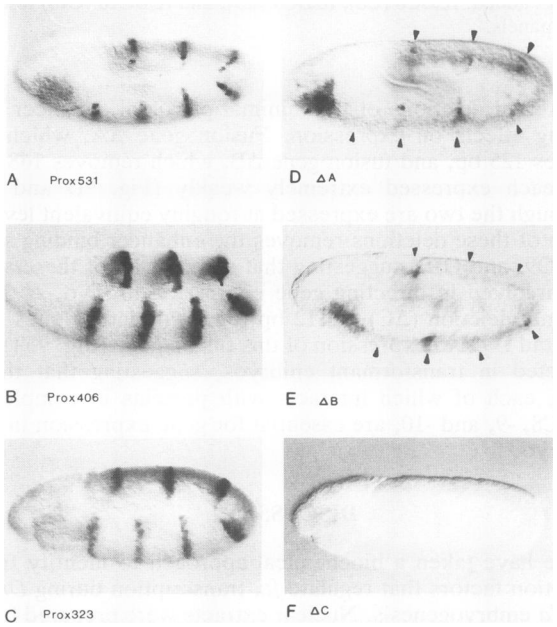

FIG. 9. Expression of *ftz* proximal enhancer-*lacZ* fusion genes. Transformant embryos carrying the indicated *lacZ* fusion genes were stained by immunohistochemical methods to detect β-galactosidase expression. All embryos are named according to the DNA construct with which they were transformed. Embryos are oriented anterior to the left and dorsal side up. All embryos are at the germ band extension stage. Fusion genes Prox 531 (A), Prox406 (B), and Prox323 (C) are expressed in seven *ftz*-like stripes; ΔA (D) and ΔB (E) are expressed very weakly and ΔC (F) has no detectable expression. Arrows in panels D and E indicate the positions of the seven stripes. The apparently higher level of expression of Prox 406 compared with that in Prox 531 and Prox 323 is due to variations in the level of fusion gene expression in independent transformant lines and is not considered significant.

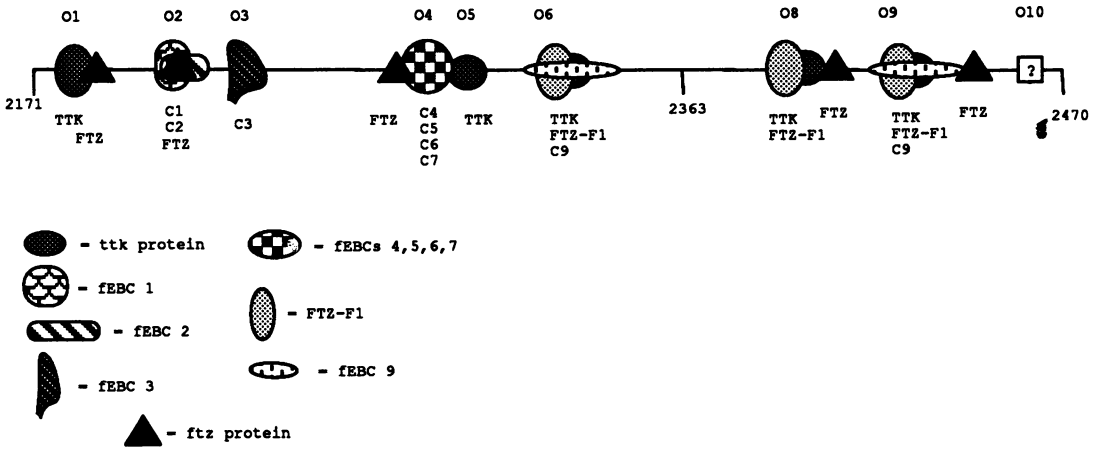

FIG. 10. An array of proteins interact with the *ftz* proximal enhancer. A schematic depiction of the newly identified fEBCs interdigitated with the previously identified *ftz* protein binding sites (30) in the minimal ~300-bp proximal enhancer is shown. The oligonucleotides that were used as probes (O1 to O6 and O8 to O10) are indicated above the line. Position 2363 indicates the previously identified breakpoint in the enhancer that separates the two interacting elements, Prox A and Prox B (30). The proteins that interact with each oligonucleotide are indicated below the line. fEBC10, which was shown to contain TTK protein (Fig. 7), is labeled TTK; similarly, fEBC8, which appears to contain FTZ-F1, is labeled FTZ-F1, although other proteins may also be present in these complexes. The five previously identified binding sites for *ftz* protein are indicated. The one high-affinity site (2198 to 2215) in the enhancer overlaps with site O2; of the three medium-affinity sites identified, one (2177 to 2195) overlaps with site O1; one (2263 to 2278) overlaps partially with O4, and one (2400 to 2426) overlaps partially with site O8. One low-affinity binding site (2435 to 2416) overlaps partially with site O9. Thus, with the exception of site O2, fEBC proteins and *ftz* protein could co-occupy sites in the enhancer. Note that sites O6 and O9 generate the same complexes in gel retardation assays. No complexes were identified for site O10 in gel retardation assays.

actually regulate *ftz* in vivo awaits purification of the proteins and isolation of the genes encoding them.

fEBC sites interdigitate with *ftz* protein binding sites. Previous studies have demonstrated that the homeodomain of the *ftz* protein, synthesized in *E. coli*, can bind to the proximal enhancer. The minimal proximal enhancer fragment identified in our studies contains one high-affinity, three medium-affinity, and one low-affinity binding sites (Fig. 10) (30). Site O2 overlaps almost exactly with the single high-affinity *ftz* binding site in this enhancer. Mutations in the ATTA core homeodomain binding site of site 2 abolished fEBC1 and -2 complex formation in gel retardation assays (data not shown). However, attempts to determine directly whether or not *Drosophila ftz* protein is present in these complexes by using either polyclonal or monoclonal anti-FTZ antibodies were inconclusive. Therefore, we do not yet know whether or not *ftz* protein in the nuclear extracts was detected in our system or, if so, if it binds to DNA with the same specificity as the *E. coli*-synthesized protein. Similarly, we do not know yet if any fEBC binds to DNA in conjunction with *ftz* protein. For example, sites O1, O4, O8, and O9, which partially overlap with the *ftz* protein binding sites, could all presumably be occupied by an fEBC and a neighboring molecule of *ftz* protein. These interactions could be either cooperative, to stimulate transcription, or mutually exclusive, with an fEBC(s) displacing *ftz* protein to turn off transcription in the stripes at the end of germ band extension. To address these questions, purification of the fEBCs is under way.

More recent studies by Schier and Gehring identified regions within the proximal enhancer that are necessary for enhancer-*lacZ* fusion genes in transgenic embryos (34). In these experiments, single or multiple *ftz* protein binding regions were deleted or mutated. Interestingly, three (ΔA, ΔB, and ΔC) of the four deletions that they created also remove fEBC binding sites. ΔA is a 78-bp deletion that removes both site 1 and site 2, along with two medium-affinity and one high-affinity *ftz* binding sites; ΔB is a 10-bp deletion that removes part of site 4 and one medium-affinity *ftz* binding site; ΔC is a 24-bp deletion that removes the entire site 8 and a neighboring *ftz* medium-affinity site. The fourth deletion of 32 bp (ΔD) removes a region found to be dispensable in our studies. These deletions leave one low-affinity *ftz* binding site (2437 to 2452) unaffected. None of these deletions had a significant effect on *lacZ* expression when tested alone; however, in combination, multiple deletions reduced expression significantly. Since our preliminary results indicate that point mutations in multiple fEBC binding sites also reduce expression of *lacZ* fusion genes in vivo (data not shown), it is possible that the effects seen in their experiments (34) were at least partially due to deletion of fEBC binding sites. We are in the process of creating *lacZ* fusion genes with mutations in individual binding sites to distinguish these possibilities.

The biochemical approach. We have taken a biochemical approach to complement the genetic analyses that have identified potential regulators of the *ftz* gene. Although these analyses have made the study of gene regulation during embryonic development possible by identifying a large number of genes required for normal development (21, 26, 27), not all embryonically active genes were identified in genetic screens. Classes of genes that would not have been identified in mutant screens include redundant or duplicated genes, genes with complementary maternal and zygotic functions, haplo-insufficient genes, genes affecting only internal structures of the embryo, genes whose mutation causes developmental arrest before cuticular development, and genes whose mutation results in subtle phenotypes or has dominant lethal affects (19). Examples of genes encoding putative transcription factors missed in the screens that have subsequently been identified by other methods are the homeobox-containing gene *caudal* (25), *Drosophila AP-1* (28), *pox meso*

and *pox neuro* (3), and the *ftz* regulatory genes encoding FTZ-F1 and tramtrack/FTZ-F2 (12, 20). Thus, it is clear that a variety of approaches will be necessary to fully understand the complex regulatory networks that control embryonic development.

The *ftz* zebra and upstream enhancer elements have been the subjects of biochemical studies with embryo extracts (4, 8, 11, 12, 20, 38, 39). Harrison and Travers (11) conducted a direct DNase I footprinting assay on the whole *ftz* upstream element by using crude embryo nuclear extracts. In the proximal enhancer, nearly all (70%) of the sequence was footprinted. Some footprint sites were over 100 bp long. However, no evidence was provided to identify the specific DNA-protein interactions responsible for these extended footprints. Eight of the nine footprint sites (except site 10) identified in our study lie within these previously identified sites. This overlap suggests that our footprint sites are the core sequences that interact specifically with DNA-binding proteins.

FTZ-F1 and TTK-FTZ-F2 are potential *ftz* regulatory proteins. The *ttk* gene encodes a DNA-binding protein with a zinc finger motif (4, 11). Two TTK/FTZ-F2 binding sites were found in the *ftz* zebra element. Mutation of these binding sites led to premature and ectopic expression of *lacZ* fusion genes in transgenic embryos (4). Ectopic expression of TTK/FTZ-F2 throughout the embryo resulted in a severe disruption of *ftz* expression (32). These studies suggest that TTK/FTZ-F2 functions as a repressor of *ftz* transcription. The FTZ-F1 gene encodes a member of the hormone receptor superfamily (20). Two DNA-binding sites were found in the zebra element, which, when mutated, led to loss of striped expression, particularly in stripes 2, 3, and 6. This observation suggested that FTZ-F1 is a transcriptional activator of *ftz* expression that may have stripe-specific effects.

We have defined five new TTK/FTZ-F2 binding sites and three FTZ-F1 binding sites in the *ftz* proximal enhancer. In total, 11 TTK/FTZ-F2 binding sites have been identified in *ftz* regulatory elements: 5 in the proximal enhancer (this report), 1 in the region between the proximal and distal enhancers (12), and 5 in the zebra element (4, 12). Likewise, five FTZ-F1 binding sites have now been described: three in the proximal enhancer (this report) and two in the zebra element (39). Interestingly, four of the TTK/FTZ-F2 binding sites overlap four FTZ-F1 binding sites: proximal enhancer sites 6, 8, and 9 and the zebra element FTZ-F1 binding site II (39). We propose that these two proteins with opposite functions compete for the same set of DNA-binding sites in vivo. This process may be one mechanism for the rapid activation and repression of *ftz* transcription in stripes in the developing embryo.

ACKNOWLEDGMENTS

We are grateful to Lesley Brown, Giovanni Lavorgna, and Carl Wu for providing us with anti-FTZ-F1 and FTZ-F2/TTK antibodies and to Douglas Read and James Manley for the bacterially expressed TTK protein and for anti-TTK antibodies. The manuscript was greatly improved by the comments of Barbara Ruskin. L.P. expresses her sincere appreciation to Walter J. Gehring for supporting the development of the in vitro transcription system in his laboratory.

This work was supported in part by a grant from the National Institutes of Health (HD 27937-01A1). L.P. was a recipient of an Alexandrine and Alexander L. Sincheimer Award and an Irma T. Hirschl Career Scientist Award.

REFERENCES

1. **Akam, M.** 1987. The molecular basis for metameric pattern in the *Drosophila* embryo. Development **101**:1–22.
2. **Biggin, M. D., and R. Tjian.** 1988. Transcriptional factors that activate the *Ultrabithorax* promoter in developmentally staged extracts. Cell **53**:699–711.
3. **Bopp, D., E. Jamet, S. Baumgartner, M. Burri, and M. Noll.** 1989. Isolation of two tissue-specific *Drosophila* paired box genes, *pox meso* and *pox neuro*. EMBO J. **8**:3447–3457.
4. **Brown, J. L., S. Sonoda, H. Ueda, M. P. Scott, and C. Wu.** 1991. Repression of the *Drosophila fushi tarazu* (*ftz*) segmentation gene. EMBO J. **10**:665–674.
5. **Carroll, S. B., and M. P. Scott.** 1985. Localization of *fushi tarazu* protein during *Drosophila* embryogenesis. Cell **43**:47–57.
6. **Carroll, S. B., and M. P. Scott.** 1986. Zygotically active genes that affect the spatial expression of the *fushi tarazu* segmentation gene during early *Drosophila* embryogenesis. Cell **45**:113–126.
7. **Carthew, R. W., L. A. Chodosh, and P. A. Sharp.** 1985. An RNA polymerase II transcription factor binds to an upstream element in the adenovirus major late promoter. Cell **43**:439–448.
8. **Dearolf, C. R., J. Topol, and C. S. Parker.** 1989. Transcriptional control of *Drosophila fushi tarazu* zebra stripe expression. Genes Dev. **3**:384–398.
9. **Dearolf, C. R., J. Topol, and C. S. Parker.** 1990. Transcriptional regulation of the *Drosophila* segmentation gene *fushi tarazu* (*ftz*). Bioessays **12**:109–113.

9a. **Gutjahr, T.** Personal communication.

10. **Hafen, E., A. Kuroiwa, and W. J. Gehring.** 1984. Spatial distribution of transcripts from the segmentation gene *fushi tarazu* during Drosophila embryonic development. Cell **37**:833–841.
11. **Harrison, S. D., and A. Travers.** 1988. Identification of the binding sites for potential regulatory proteins in the upstream enhancer element of *Drosophila fushi tarazu* gene. Nucleic Acids Res. **16**:11403–11416.
12. **Harrison, S. D., and A. Travers.** 1990. The *tramtrack* gene in *Drosophila* encodes a zinc finger protein that interacts with the *ftz* transcriptional regulatory region and shows a novel embryonic expression pattern. EMBO J. **9**:207–216.
13. **Hendrickson, W., and R. Schleif.** 1985. A dimer of AraC protein contacts three adjacent major groove regions at the AraI DNA site. Proc. Natl. Acad. Sci. USA **82**:3129–3133.
14. **Hiromi, Y., and W. J. Gehring.** 1987. Regulation and function of the *Drosophila* segmentation gene *fushi tarazu*. Cell **50**:963–974.
15. **Hiromi, Y., A. Kuroiwa, and W. J. Gehring.** 1985. Control elements of the *Drosophila* segmentation gene *fushi tarazu*. Cell **43**:603–613.
16. **Ingham, P., and P. Gergen.** 1988. Interactions between the pair-rule genes *runt*, *hairy*, *even-skipped* and *fushi tarazu* and the establishment of periodic pattern in the *Drosophila* embryo. Development **104**(Suppl.):51–60.
17. **Ingham, P. W.** 1988. The molecular genetics of embryonic pattern formation in *Drosophila*. Nature (London) **335**:25–34.
18. **Johnston, D. S., and C. Nusslein-Volhard.** 1992. The origin of pattern and polarity in the *Drosophila* embryo. Cell **68**:201.
19. **Jurgens, G., E. Wieschaus, C. Nusslein-Volhard, and H. Kluding.** 1984. Mutations affecting the pattern of the larval cuticle in *Drosophila melanogaster*. II. Zygotic loci on the third chromosome. Wilhelm Roux Arch. Dev. Biol. **193**:283–295.
20. **Lavorgna, G., H. Ueda, J. Clos, and C. Wu.** 1991. FTZ-F1, a steroid hormone receptor-like protein implicated in the activation of *fushi tarazu*. Science **252**:848–851.
21. **Lewis, E. B.** 1978. A gene complex controlling segmentation in *Drosophila*. Nature (London) **276**:565–570.
22. **Maniatis, T., E. F. Fritsch, and J. Sambrook.** 1982. Molecular cloning: a laboratory manual. Cold Spring Harbor Laboratory, Cold Spring Harbor, N.Y.
23. **Maxam, A. M., and W. Gilbert.** 1977. A new method for sequencing DNA. Proc. Natl. Acad. Sci. USA **74**:560–564.
24. **Maxam, A. M., and W. Gilbert.** 1980. Sequencing end-labeled DNA with base specific chemical cleavages. Methods Enzymol. **65**:409–560.

25. **Mlodzik, M., and W. J. Gehring.** 1987. Expression of the *caudal* gene in the germ line of *Drosophila*: formation of an RNA and protein gradient during early embryogenesis. Cell **48**:465–478.
26. **Nusslein-Volhard, C., and E. Wieschaus.** 1980. Mutations affecting segment number and polarity in *Drosophila*. Nature (London) **287**:795–801.
27. **Nusslein-Volhard, C., E. Wieschaus, and H. Kluding.** 1984. Mutations affecting the pattern of the larval cuticle in *Drosophila melanogaster*. I. Zygotic loci on the second chromosome. Wilhelm Roux Arch. Dev. Biol. **193**:267–282.
28. **Perkins, K. K., A. Admon, N. Patel, and R. Tjian.** 1990. The *Drosophila* Fos-related AP-1 protein is a developmentally regulated transcription factor. Genes Dev. **4**:822–834.
29. **Perkins, K. K., G. M. Dailey, and R. Tjian.** 1988. In vitro analysis of the *Antennapedia* P2 promoter: identification of a new *Drosophila* transcription factor. Genes Dev. **2**:1615–1626.
29a. **Pick, L.** Unpublished data.
30. **Pick, L., A. Schier, M. Affolter, T. Schmidt-Glenewinkel, and W. J. Gehring.** 1990. Analysis of the *ftz* upstream element: germ layer-specific enhancers are independently autoregulated. Genes Dev. **4**:1224–1239.
31. **Read, D., T. Nishigaki, and J. L. Manley.** 1990. The *Drosophila even-skipped* promoter contains multiple, overlapping factor binding sites and is transcribed in a stage-specific manner in vitro. Mol. Cell. Biol. **10**:4334–4344.
32. **Read, D. B.** 1992. Expression and function of the *tramtrack* gene of *Drosophila*. PhD thesis. Columbia University, New York.
33. **Rubin, G. M., and A. C. Spradling.** 1982. Genetic transformation of *Drosophila* with transposable element vectors. Science **218**:348–353.
34. **Schier, A. F., and W. J. Gehring.** 1992. Direct homeodomain-DNA interaction in the autoregulation of the *fushi tarazu* gene. Nature (London) **356**:804–807.
35. **Soeller, W. C., S. J. Poole, and T. Kornberg.** 1988. In vitro transcription of the *Drosophila engrailed* gene. Genes Dev. **2**:68–81.
36. **Spradling, A. C., and G. M. Rubin.** 1982. Transposition of cloned P element into *Drosophila* germ line chromosomes. Science **218**:341–347.
37. **Staudt, L. M., and M. J. Lenardo.** 1991. Immunoglobulin gene transcription. Annu. Rev. Immunol. **9**:373–398.
38. **Topol, T., C. R. Dearolf, K. Prakash, and C. S. Parker.** 1991. Synthetic oligonucleotide recreate *Drosophila fushi tarazu* zebra-stripes expression. Genes Dev. **5**:855–867.
39. **Ueda, H., S. Sonoda, L. Brown, M. P. Scott, and C. Wu.** 1990. A sequence-specific DNA-binding protein that activates *fushi tarazu* segmentation gene expression. Genes Dev. **4**:624–635.